Prediction of Jump Phenomena in Roll-Coupled Maneuvers of Airplanes

A. A. Schy* and M. E. Hannah†
NASA Langley Research Center, Hampton, Va.

An easily computerized analytical method is developed for identifying critical airplane maneuvers in which nonlinear rotational coupling effects may cause sudden jumps in the response to pilot's control inputs. Fifth- and ninth-degree polynomials for predicting multiple pseudosteady states of roll-coupled maneuvers are derived. The program calculates the pseudosteady solutions and their stability. The occurrence of jump-like responses for several airplanes and a variety of maneuvers is shown to correlate well with the appearance of multiple stable solutions for critical control combinations. The analysis is extended to include aerodynamics nonlinear in angle of attack.

Introduction

PHILLIPS'[1] original analysis of the roll-coupling problem considered the rotational coupling effects of constant roll rate on the stability of the short-period longitudinal and lateral oscillations. Although the constant rolling constraint is artificial, it is physically realistic for well-behaved airplanes with good damping in roll. Phillips' analysis predicted that divergence-like motions would be expected at certain critical roll rates, when the usual linearized stability analysis predicted perfectly acceptable behavior. This dangerous coupling effect of rapid rolling, leading to large deviations in incidence angles and tail loads, was confirmed in many nonlinear computerized simulations and in flight. In connection with these simulation studies, there were many attempts to extend Phillips' analysis. The main objective of these studies was to obtain a simplified method for predicting the peak motions in roll-coupled maneuvers.

Pinsker[2] and Rhoads and Schuler[3] showed that Phillips' critical roll rates also could be obtained as steady-state (autorotational) solutions of the approximate equations of motion used by Phillips. This method has the advantages that it also predicts steady-state solutions for the other variables, is more readily generalized, and permits the use of control input values as independent parameters, instead of roll rate. However, attempts to use this method to predict peak disturbances reliably in coupled maneuver were not successful. In the present study we have returned to this method of calculating the steady states of the approximate equations of motion, which we shall call the pseudosteady-state (PSS) method, because it neglects the effects of varying weight components in body axes. However, instead of trying to predict the magnitudes of response peaks, the method will be used to predict those control input combinations that may cause sudden "jumps" in the response as the motion is "attracted" to a new stable pseudosteady-state.

Preliminary Remarks

A recent paper,[4] which presents an excellent review of past work on roll coupling, also shows that it is necessary to include gravity effects to predict peaks in the response. The authors introduce an expansion using g/V as a small parameter, and calculate approximate oscillatory control deflection requirements to enforce the artificial constraint of constant roll rate. By use of these special control inputs, they show that their approximate expansion, including first-order weight effects, fits the peaks of the integrated equations well. Another recent paper[5] has shown that, for any arbitrary time-varying roll-rate, the other responses can be predicted using an expansion in $p(t)$. However, the difficulty with these types of analysis, which depend on specifying the form of roll rate, is that in nonlinear maneuvers there is no *a priori* way to predict the roll-rate response. Simulator studies of maneuvering airplanes have shown that certain combinations of constant control deflections can lead to very sudden and irregular "jump-like" responses in all variables, including roll rate.

In order to illustrate this, Fig. 1 shows the roll-rate responses to two rectangular-pulse aileron inputs for the fighter airplane sample flight condition used in Ref. 5. The dotted lines show the $p(t)$ responses assumed in this reference after the aileron is centered. Even for the 5° aileron, the calculated response is substantially different; whereas for the 10° pulse the roll rate does not even return to zero, but "jumps" into an autorotational state. All of the complicated response calculations in Ref. 5 for the assumed $p(t)$ in this critical range therefore are useless, since they would never occur in an actual rolling maneuver unless the controls were moved in a complicated manner not known to the pilot.

In the present study, the control inputs are the independent variables instead of the roll rate. An analytical solution for the pseudosteady-state corresponding to any combination of control inputs is derived, along with the linear perturbation characteristic polynomial defining the stability of the pseudosteady maneuver. The existence of multiple stable

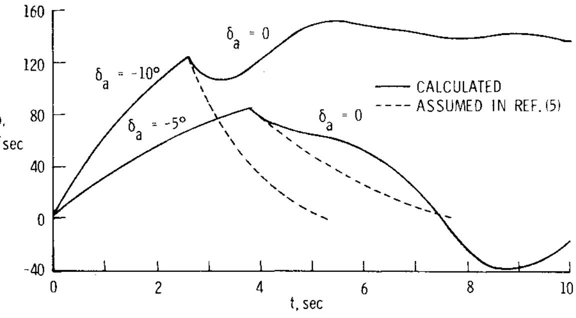

Fig. 1 Comparison of calculated roll-rate response to rectangular aileron pulse and roll rate assumed in Ref. 5.

Presented at the AIAA 3rd Atmospheric Flight Mechanics Conference, Arlington, Texas, June 7-9, 1976 (in bound volumes of Conference papers, no paper number); submitted June 25, 1976; revision received Nov. 29, 1976.

Index category: Aircraft Handling, Stability, and Control.

*Supervisory Aerospace Engineer. Associate Fellow AIAA.
†Aerospace Engineer.

solutions at any combination of control deflections is assumed to be a necessary condition for the occurrence of a jump in the response, resulting from the nonlinear rotational coupling effects. The identification of such critical control combinations is the main role of the approximate PSS analysis. Comparison of the PSS results to integrated time histories for a number of examples indicates that various types of jump phenomena can be predicted. In order to obtain accurate peak responses, the complete nonlinear equations of motion can be used for the critical conditions identified by the PSS analysis. Although results are presented only for linear aerodynamics, the analysis is extended to include aerodynamics nonlinear in α.

Analysis

The approximate nonlinear equations of motion are presented in Appendix A. These were used to calculate all time histories in this paper. They assume that speed is constant, that the incidence angles (α and β) are small as compared to one radian, and that aerodynamics are linear. Principal axes are used. Seven first-order equations result. The stability of the linearized perturbed motion from any equilibrium solution to these equations is determined by a seventh-order characteristic equation. In order to obtain an equilibrium or steady-state solution, it is necessary to solve the nonlinear equations that result when all time derivatives are set equal to zero. By use of modern computers and algorithms, this can be done even for the complete equations and nonlinear aerodynamics, with no simplifying assumptions; however, it is known that such solutions must be spiral paths about a vertical axis, because of the vertical weight force.[6] Since the sudden jump phenomena of concern in this study seem unrelated to such vertical spirals, but seem rather to be related to the rotational coupling effects at any orientation, the PSS approach is to ignore the variation of body-axis components of weight, in order to eliminate the constraint that the rotational velocity be vertical. The resulting equations for the PSS solutions are obtained by dropping the g/V terms in the force equations (which depend on ϕ and θ) and the associated $\dot{\phi}$ and $\dot{\theta}$ equations, and setting the time derivative terms in the other five equations to zero.

Solution for Pseudosteady States

Leaving aside the rolling equation, the other four equations are linear in $\bar{q}$, $\bar{r}$, $\bar{\beta}$, and $\overline{\Delta\alpha}$, where the bars indicate PSS solutions. These can be written as

$$\bar{p}\bar{q} - \hat{n}_r\bar{r} - \hat{n}_\beta\bar{\beta} = \hat{n}_{\delta a}\delta_a + \hat{n}_{\delta r}\delta_r + \hat{n}_p\bar{p} \tag{1}$$

$$\hat{m}_q\bar{q} + \bar{p}\bar{r} + \hat{m}_\alpha\overline{\Delta\alpha} = -\hat{m}_{\delta e}\delta_e \tag{2}$$

$$-\bar{q} + \bar{p}\bar{\beta} - z_\alpha\overline{\Delta\alpha} = z_{\delta e}\delta_e \tag{3}$$

$$-\bar{r}\cos\alpha_0 + y_\beta\bar{\beta} + \bar{p}\overline{\Delta\alpha} = -y_{\delta a}\delta_a - y_{\delta r}\delta_r - \bar{p}\sin\alpha_0 \tag{4}$$

In vector-matrix form, defining $x^T(\bar{p}) = \bar{q}, \bar{r}, \bar{\beta}, \overline{\Delta\alpha})$, these equations take the form

$$(\bar{p}I_4 - M)x = c + \bar{p}b \tag{5}$$

Where I_4 is the fourth-order identity

$$M = \begin{bmatrix} 0 & \hat{n}_r & \hat{n}_\beta & 0 \\ -\hat{m}_q & 0 & 0 & -\hat{m}_\alpha \\ 1 & 0 & 0 & z_\alpha \\ 0 & \cos\alpha_0 & -y_\beta & 0 \end{bmatrix} \tag{6}$$

$$c^T = (\hat{n}_c, -\hat{m}_c, z_c, -y_c) \tag{7}$$

and

$$b^T = (\hat{n}_p, 0, 0, -\sin\alpha_0) \tag{8}$$

The vector c and subscript c indicate the control input terms. The solution of Eq. (5) is

$$x(\bar{p}) = (\bar{p}I_4 - M)^{-1}(c + \bar{p}b) \tag{9}$$

The inverse matrix in Eq. (9) is in the same form that occurs in the Laplace transform solution of a set of four first-order differential equations, and is a matrix of rational functions of $\bar{p}$. By use of the numerical values for M, c, and b, the solution for Eq. (9) is programmed easily for computer calculation, giving solutions $\bar{q}(\bar{p})$, $\bar{r}(\bar{p})$, $\bar{\beta}(\bar{p})$, and $\overline{\Delta\alpha}(\bar{p})$ in the form

$$x_i(\bar{p}) = N_i(\bar{p})/Q(\bar{p}^2) \tag{10}$$

Here $Q(\bar{p}^2)$ is the quartic expression obtained by evaluating $|\bar{p}I_4 - M|$, which turns out to be quadratic in $\bar{p}^2$.

$$Q(\bar{p}^2) = \bar{p}^4 + (\hat{m}_\alpha\cos\alpha_0 - \hat{n}_\beta + z_\alpha y_\beta + \hat{m}_q\hat{n}_r)\bar{p}^2$$
$$-(\hat{m}_\alpha - z_\alpha\hat{m}_q)(n_\beta\cos\alpha_0 + y_\beta\hat{n}_r) \tag{11}$$

Positive solutions of $Q(\bar{p}^2) = 0$ define critical values of $\bar{p}$, since the solutions in Eq. (9) are undefined at these values. As was originally pointed out in Refs. 2 and 3, these critical PSS values correspond essentially to the critical roll rates defined by Phillips in Ref. 1. However, these values do not play an important role in the PSS analysis. The PSS solutions are obtained as follows.

Generally, when the solutions from Eq. (9) are inserted into the rolling equation

$$\hat{I}_\beta\bar{\beta} + \hat{I}_r\bar{r} + \hat{I}_p\bar{p} - \bar{q}\bar{r} + \hat{I}_{\delta a}\delta_a + \hat{I}_{\delta r}\delta_r = 0$$

The result may be written

$$\hat{I}_c + \hat{I}_p\bar{p} + f_1(\bar{p})/Q(\bar{p}^2) - f_2(\bar{p})/Q^2(\bar{p}^2) = 0 \tag{12}$$

where $\hat{I}_c$ represents the control input terms, and f_1 and f_2 are defined by the numerators of $\bar{\beta}$, $\bar{r}$, and $\bar{q}$ as

$$f_1(\bar{p}) = [\hat{I}_\beta\bar{\beta}(\bar{p}) + \hat{I}_r\bar{r}(\bar{p})]Q(\bar{p}^2) \tag{13}$$

$$f_2(\bar{p}) = [\bar{q}(\bar{p})\bar{r}(\bar{p})]Q^2(\bar{p}^2) \tag{14}$$

Note that the values of $\bar{p}$ corresponding to $Q = 0$ cannot be used in Eq. (12) to define corresponding control deflections, because of the singularity at that point. However, using the control deflections as the independent variables, $\hat{I}_c$ is well defined, and solutions of Eq. (12) give the corresponding PSS values for all variables.

Multiplying Eq. (12) by Q^2 yields a ninth-degree polynomial equation for the PSS values $\bar{p}$.

$$N(\bar{p}) = (\hat{I}_c + \hat{I}_p\bar{p})Q^2 + f_1Q - f_2 = 0 \tag{15}$$

The polynomial form is preferable for computer solution. Solutions of Eq. (15) are valid solutions of Eq. (12) if they are not solutions of $Q = 0$. If they do occur, for isolated control values, at $Q = 0$ solutions, then they must be multiple roots of Eq. (15) to be valid solutions of Eq. (12). No such solutions have occurred in the examples considered in this paper.

In most roll-coupling studies, the last term in Eq. (12) is neglected, assuming the product $\bar{q}\bar{r}$ to be of minor influence. The fifth-degree polynomial for PSS solutions $\bar{p}$ then becomes

$$V(\bar{p}) = (\hat{I}_c + \hat{I}_p\bar{P})Q + f_1 = 0 \tag{16}$$

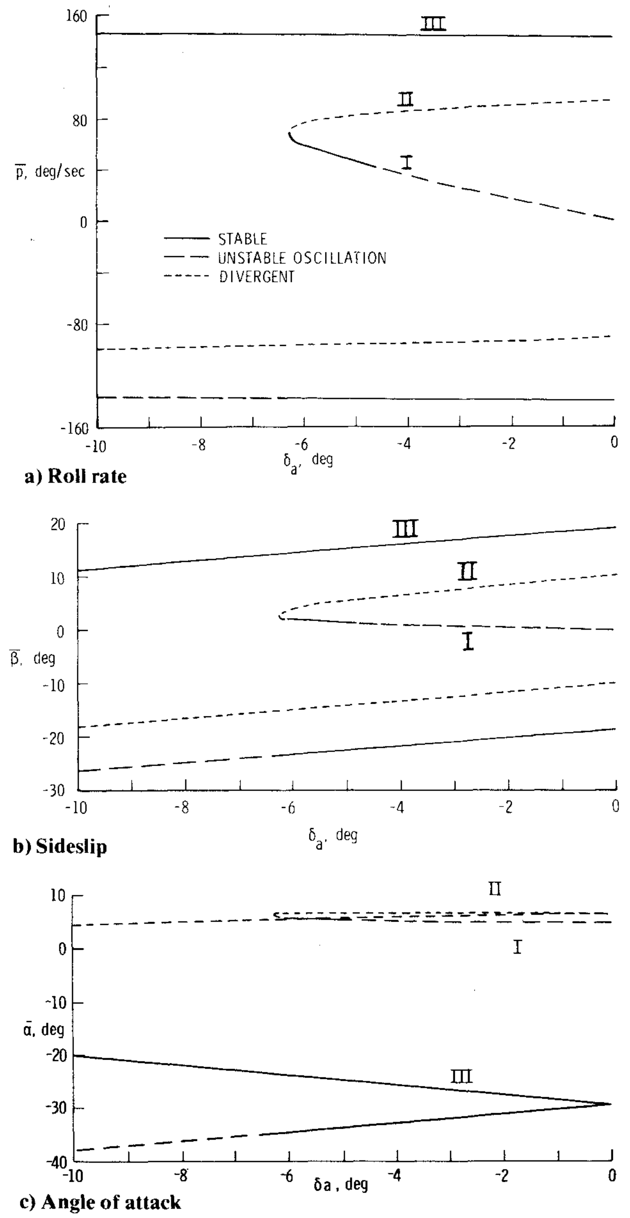

Fig. 2 PSS solutions for fighter airplane example of Ref. 5, airplane A, aileron only.

Again, solutions of Eq. (16) are valid for the truncated Eq. (12) only if they are multiple solutions. In some cases, solutions of Eq. (16) have occurred at solutions of $Q=0$. However, these were not multiple roots, and the time histories of the responses for these control inputs showed no jump phenomena, as expected. Solutions of Eq. (16) seem to be adequately accurate in the examples used in this paper, if points near $Q=0$ solutions are eliminated. In these examples, the main difference between ninth- and fifth-degree solutions has been the introduction of four extra roots for Eq. (15), which practically are invariant with input, very near the four $Q=0$ solutions. These extra solutions seem to be asymptotes for the more significant fifth-degree solutions. Therefore, except for one example, only results of the fifth-degree equation are presented.

Although all of the results in this paper are based on the assumption of linear aerodynamics, since the existence of the jump phenomena is assumed to result from the rotational coupling terms, it is clear that when large deviations in α occur, it would be desirable to include aerodynamic effects nonlinear in α. Therefore, the analysis has been extended to include aerodynamic effects that are nonlinear in α and control deflections. The polynomial in $\bar{p}$ is replaced by two equations in $\bar{p}$ and $\bar{\alpha}$ which should be solvable easily on the computer. This analysis is presented in Appendix B.

Stability of PSS Solutions

The stability of the PSS solutions was calculated by inserting PSS solutions into the corresponding five equations of motion in Appendix A and linearizing about the PSS values. The matrix whose characteristic roots determine the stability of the perturbed motion is

$$A=\begin{bmatrix} y_\beta & \bar{p} & \sin\bar{\alpha} & 0 & -\cos\bar{\alpha} \\ -\bar{p} & z_\alpha & -\bar{\beta} & 1 & 0 \\ l_\beta & 0 & l_p & -J_x\bar{r} & l_r-J_x\bar{q} \\ 0 & m_\alpha & J_y\bar{r} & m_q & J_y\bar{p} \\ n_\beta & 0 & n_p-J_z\bar{q} & -J_z\bar{p} & n_r \end{bmatrix} \tag{17}$$

where

$$J_x=\frac{I_z-I_y}{I_x}\qquad J_y=\frac{I_z-I_x}{I_y}\qquad J_z=\frac{I_y-I_x}{I_z}$$

Note the absence of the hats on the moment derivatives in A. The inertia ratios are not factored out as in Appendix A.

The stability of the PSS solutions is an essential factor in predicting control inputs for which jump phenomena may occur. The digital program, which calculates the PSS solutions for any combination of control inputs, by using the appropriate values for $\hat{l}_c$ in Eq. (15) and/or Eq. (16) and $\hat{m}_c$, $\hat{n}_c$, y_c, and z_c in Eq. (9), also calculates characteristic roots of Eq. (17). The PSS solution may be multiple valued for some ranges of control input. That branch of the solution which starts at $\bar{p}=0$ for zero lateral inputs is called the "basic solution" branch. It is assumed that jumps in the response may occur when another stable branch exists. A solution that is stable except for a slightly unstable oscillation is assumed to act as a stable "attractor" (it effectively has a "positive spring constant"). Also, the approximations in the PSS analysis imply a corresponding uncertainty in the stability prediction, so that it is not feasible to distinguish between slightly stable or unstable modes. In fact, the stability effects of the varying weight components are neglected in Eq. (17), so that only fifth-order approximate characteristics are obtained.

Results and Discussion

The method has been applied to a number of examples. Results will be shown for four airplanes. The first of these is a well-known fighter airplane flight condition, which was used in most of the earlier studies. It also was used as the example in Ref. 5. The second case was taken from Etkin's text on flight dynamics.[7] In this example, a pitch-down elevator is assumed along with the aileron, and the coupled maneuver is markedly different from the first example. The third and fourth cases are another fighter airplane and an attack airplane. Table 1 lists the example cases presented.

Airplane A

It already has been shown in Fig. 1 that, for the case of the aileron-roll maneuver in airplane A, the roll rate tends to jump into an autorotation for some aileron inputs. Figure 2 shows the $\bar{p}$, $\bar{\alpha}$, and $\bar{\beta}$ PSS solutions. Solid lines and long dashed lines should be considered to be potential "attractor" states. The curves marked I are the basic solution. For small aileron inputs, the basic solution in Fig. 2 shows a linear variation of $\bar{p}$ with δ_a, small $\bar{\beta}$, and $\bar{\alpha}$ remaining near the trim value. However, at around 6° of aileron the basic solution

Table 1 Parameters of example airplanes

	Dynamic pressure, lb/ft^2	V, ft/sec	I_{XP}, slug-ft^2	I_{YP}, slug-ft^2	I_{ZP}, slug-ft^2	ω_θ, rad/sec	ω_ψ, rad/sec
Airplane A	197.0	691	10,976	57,100	64,975	2.417	1.83
Airplane B	297.3	500	1,700	12,400	13,600	2.17	4.44
Airplane C	86.0	269	12,000	171,000	180,000	1.661	1.01
Airplane D	75.3	317	13,476	58,966	67,719	1.713	1.65

disappears. Therefore, the PSS analysis predicts that this is a critical range of aileron values, that the roll rate and sideslip may "jump" to large values near stable solution III, and that α may jump to large negative values.

Figure 3 shows corresponding time histories obtained by integrating the equations of Appendix A for three constant aileron values. In fact, the jumps predicted for all three variables are seen to occur, although the critical aileron magnitude is near 5°, rather than 6°. In this case, the peak values are also predicted reasonably well, but this is not to be expected generally, since the neglected weight effects can have a very important influence on peak responses. The tic marks, showing where various bank angles are reached, are used to indicate the realistic part of the maneuver. In roll-coupling studies, 360° rolls usually are assumed to represent a realistic limit on the maneuver.

In this case, the PSS method seems to predict both the critical aileron input and the jump maneuver rather well. Note that the usual method of predicting the critical aileron level, using Phillips' critical roll rate ($p=\omega_\psi=1.83$ rad/sec from Table 1) and the simplified $p/\delta_a=(2V/b)\ (C_{l\delta a}/C_{pp})$, would give $\delta_a \approx 15°$.

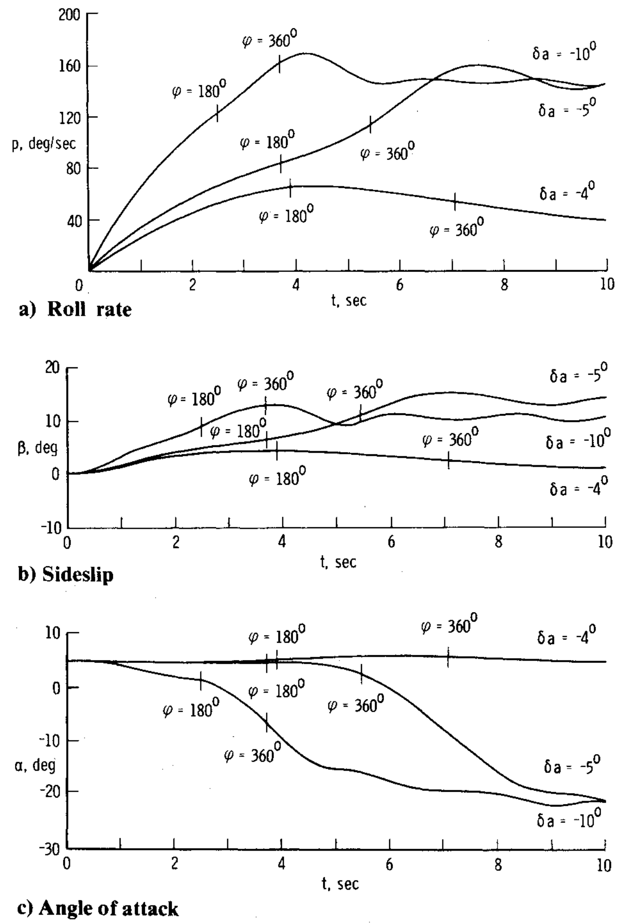

Fig. 3 Calculated responses of airplane A for several aileron inputs. Tics mark where certain bank angles are reached.

Airplane B

In this case, Etkin has considered a small jet airplane and shown that a combined pitch-down maneuver and a small aileron input can lead to a very different kind of divergence, although roll coupling is still the dominant effect.[7] For the standard aileron roll, high angle of attack aggravates the problem, since it converts into a large sideslip in the rapid roll.

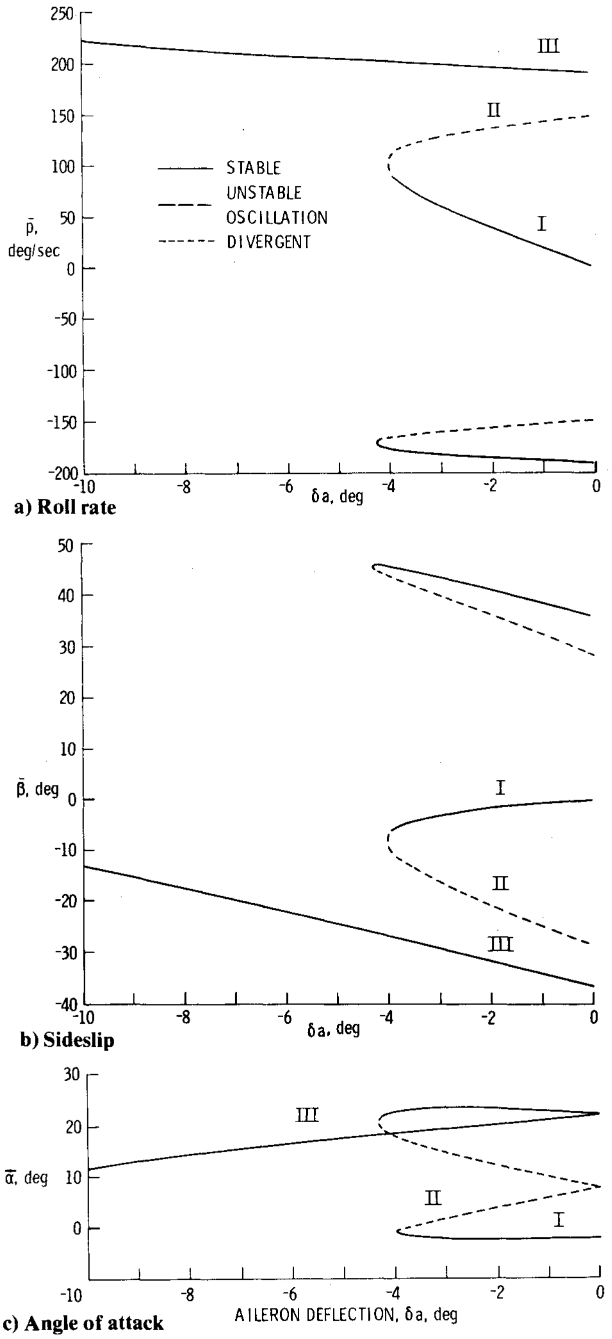

Fig. 4 PSS solutions for small jet with pitch-down elevator for airplane B, $\delta_e=2$.

In this example, the pitch down causes negative α, which converts to negative β, which, in turn, acts through the dihedral effect to cause rolling faster than the Phillips critical value. Thereafter, α diverges to large positive values; thus confirming the value of Phillips criterion, as noted by Etkin. However, the previous explanation is useful only after the problem has been observed in the time histories, since the high roll rate could not have been expected for small aileron deflections. The PSS method on the other hand, does predict that, with a 2° elevator input, a jump in the response can be expected at aileron values above 4° or 5°, as shown in Fig. 4. Essentially, the same argument as was used in the previous case for Fig. 2 with regard to the configuration of curves I, II, and III can be applied to Fig. 4. Here jumps to negative β and large positive α are predicted, along with the jump to large p.

The time histories for 4° and 5° aileron are shown in Fig. 5, and they confirm the existence and nature of the jump phenomena at the predicted critical control input values. The tendency to develop negative sideslip and the positive divergence in angle of attack after the roll rate builds up can be seen. The critical roll rate of Phillips is useful in explaining the instability leading to the divergence-like motions, but the PSS analysis shows *a priori* which critical control combinations should be studied using the complete simulator equations.

In both of these cases, the PSS analysis has predicted control inputs where jump phenomena occur in the response. Although the mechanism of the coupling was quite different, the critical condition corresponds in both cases to a disappearance of the real solution of the fifth-degree equation corresponding to the basic branch of the $\bar{p}$ vs δ_a curves. This solution combines with another (divergent) real solution to form a complex root at higher aileron values.

Airplane C

This case is a flight condition of another fighter airplane. First, the effects of applying aileron alone will be considered. For this case, the results of the ninth-degree equation will be compared with the fifth-degree results, to show why only fifth-degree results are presented in the other cases. Figure 6 shows the PSS solution, and Fig. 7 shows the associated time histories for several constant aileron deflections. For the sake of brevity, only roll-rate resuts will be shown in this and the remaining examples.

In Fig. 6, the fifth-degree solutions are practically coincident with the associated ninth-degree solutions. The four extra ninth-degree solutions are practically equal to the values for $Q=0$ and are very divergent for all values of aileron. They seem to be asymptotes for the other solutions, but otherwise played no important role in the examples considered in this investigation.

The fifth-degree solution is single valued at $\delta_a=0$, indicating that this case is not autorotational. A new stable fifth-degree solution appears as curve III at $\delta_a=-24°$, so that value is potentially critical. The roll rate may jump here from near 60°/sec to two or three times that value. The basic curve in Fig. 6 is very nonlinear for δ_a values larger than 5° in magnitude, indicating that the nonlinear rotational coupling becomes important before the critical range of aileron. This can be seen by a sort of "saturation" effect in $\bar{p}$ at these aileron magnitudes.

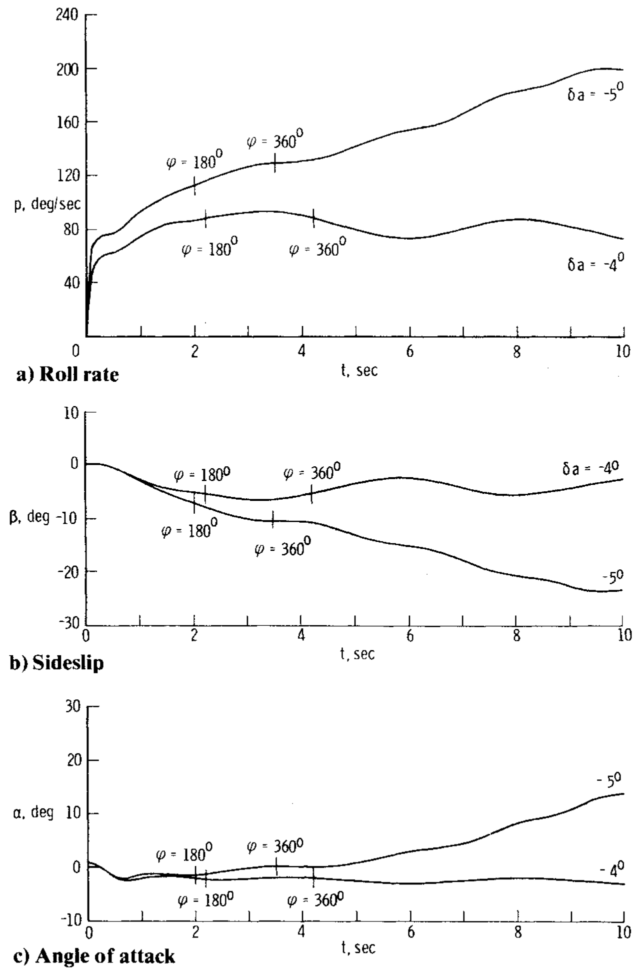

Fig. 5 Calculated responses for aileron inputs in critical range of Fig. 4.

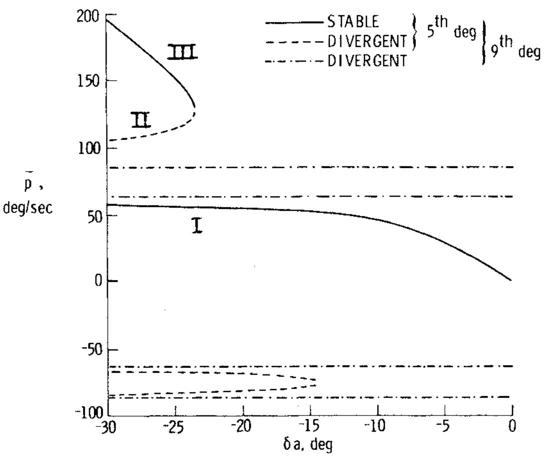

Fig. 6 Comparison of fifth-degree and ninth-degree roll-rate PSS solutions for airplane C, aileron only.

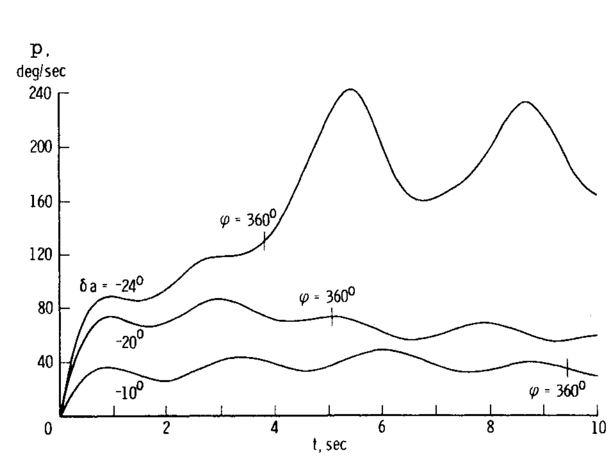

Fig. 7 Calculated roll-rate response of airplane C for several aileron inputs, $\delta_e=0$.

Referring to the time histories in Fig. 7, responses are shown for $\delta_a = -10°$, $-20°$, and $-24°$. For $\delta_a = -24°$, a violent jump in the response occurs between 3 and 4 sec. Roll rate jumps to very large positive values, as predicted, and a large, irregular oscillation appears near 200°/sec. Similar jumps and oscillations occur in the α and β responses, which are not shown. Although the aileron value where the jump phenomenon occurs is well-predicted by the PSS curves in Fig. 6, the qualitative nature of the jumps is only crudely predicted. This is not surprising, because of the importance of the large oscillatory components in the final motion. As shown by Hacker and Oprisiu,[4] these oscillations are strongly dependent on gravity effects. This can be easily verified by integrating the equations of motion neglecting the gravity terms.

Before proceeding to the next example, a final comment on the ninth-degree solutions is necessary. The fact that the ninth-degree solutions provided no significant information in the examples used in this paper does not necessarily imply that they will never be practically useful. Although the program for calculating solutions can handle rudder inputs, these have not yet been introduced. It is possible that improper rudder inputs could cause large yawing motions, which could make the qr term much more important. Also, other airplane configurations might have very different maneuver characteristics, in which the contribution of qr may be more important. On the basis of these limited results, it would be premature to dismiss the ninth-degree formulation as useless.

The next example is for the same airplane and flight condition, but shows how a pitch-down elevator input affects the response to the aileron. This control combination is similar to that considered for airplane B. The results are shown in Figs. 8 and 9.

Since there are multiple solutions at $\delta_a = 0$ in Fig. 8, an autorotation condition is predicted for the pitch-down maneuver; and the critical aileron is near $\delta_a = -4°$, where the

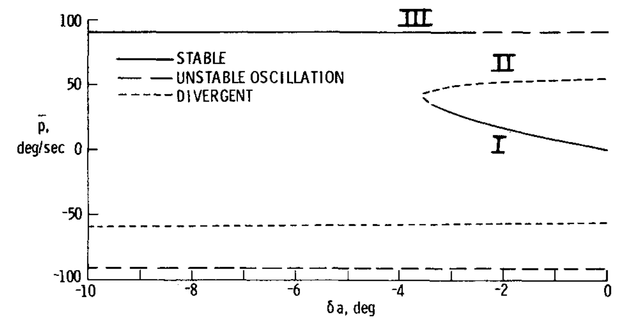

Fig. 8 Roll-rate PSS solutions of airplane C for small aileron inputs with pitch-down elevator, $\delta_e = 3°$.

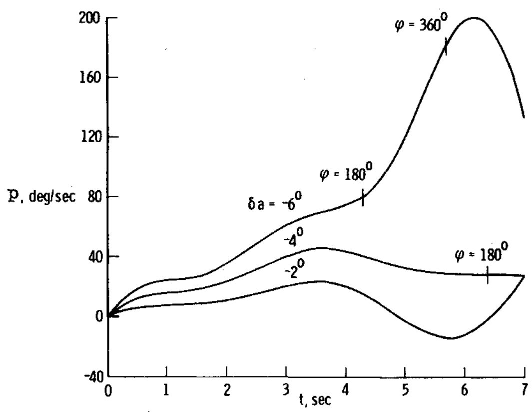

Fig. 9 Calculated roll-rate response of airplane C for small aileron inputs with pitch-down elevator, $\delta_e = 3°$.

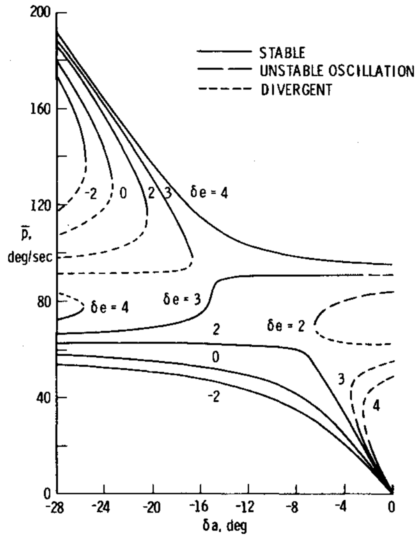

Fig. 10 Summary plot of PSS roll-rate solutions for airplane C with combined elevator and aileron inputs.

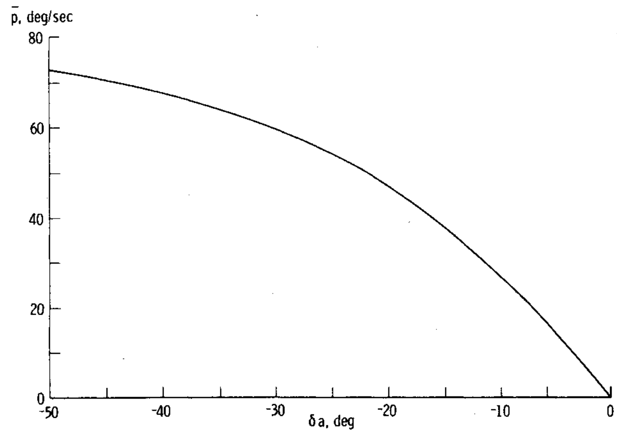

Fig. 11 Roll-rate PSS solutions of airplane D for aileron inputs.

basic solution disappears. Thus, the pitch-down maneuver has greatly decreased the critical aileron magnitude. For critical values of aileron, the roll rate should jump to large positive values. The responses in Fig. 9 show that the jump occurs for $\delta_a = -6°$, rather than at $\delta_a = -4°$. During the time interval roughly between 4 and 6 sec, as the airplane banks from 180° to 360°, the roll rate jumps to large positive values. Although the results are not shown, β takes a sharp negative jump and α takes a sharp positive jump in this same time period; and these directions are consistent with the corresponding stable solutions for curves III. As in the case for zero elevator deflection, the precise nature of the jump is affected strongly by the presence of a large oscillation, which is caused by the weight effects. The prediction that the critical aileron value becomes much smaller for the pitch-down maneuver is confirmed, however.

Figure 10 shows a summary plot for airplane C of $\bar{p}$ solutions vs δ_a for various elevator deflections. For simplicity, the negative solutions are not shown. Such plots can be generated very rapidly by the computer program. It clearly shows that $\delta_e > 0$ (pitch down) causes multiple solutions and predicted possible jump phenomena at much lower aileron deflections, and that elevator deflections as low as 2° or 3° may be critical. In fact, autorotational solutions first appear for δ_e between 1° and 2°. There are three different types of autorotational solution for pitch-down elevator, but all caused very irregular response to aileron, as in Fig. 9. Pitch-up elevator seems to increase the critical aileron value. In

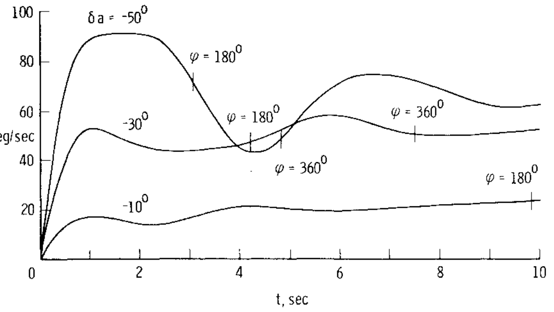

Fig. 12 Calculated roll-rate responses of airplane D for several aileron inputs.

other examples, such as airplane A, pitch-up elevator decreased the critical aileron value.

Figures 11 and 12 show PSS solutions and corresponding time histories for airplane D. These results are typical of several examples that were studied, but which showed no multiple solutions within the normal range of aileron deflection. In this case, both the PSS solutions and the time histories show that, while there are significant nonlinear coupling effects at large δ_a, no sudden jump in the response occurs. Only roll-rate response is shown in Figs. 11 and 12, but all variables approach values consistent with the PSS curves. Multiple PSS solutions actually appear at $\delta_a = 56°$, which is beyond the maximum aileron value. These results, and similar ones that were obtained for a number of other examples, show that the PSS method also reliably predicts when jumps in the response will not occur.

Finally, it should be noted that the objective in the examples shown was to cover a fairly wide range of practical cases, although an attempt was made to choose examples likely to show significant coupling effects. None of the examples, however, was studied with the thoroughness that would be necessary in practice for a specific airplane. For example, no results with rudder inputs have been shown. In a practical study, a set of cases involving all three controls and including a variety of potentially critical flight conditions would be studied. Although this would yield a mass of computer output, the calculations are very simple, can be programmed on a small computer, and require very little time. The availability of an interactive terminal and automatic plotting would be very helpful in rapid evaluation of results and elimination of unnecessary data.

Concluding Remarks

A pseudosteady-state analysis method has been described for predicting critical control input combinations, which may lead to jump phenomena in the roll-pitch response of airplanes. Calculated responses for a variety of examples have shown that jump phenomena do occur at the predicted control combinations. Future research will be aimed at generalizing the method and applying it to more detailed studies of particular airplanes, which are known to have divergent tendencies in rapid maneuvers at high angles of attack. The effects of rudder inputs will be included, and the importance of the qr term effects will be evaluated in a wider variety of maneuvers. The extension of the method to include nonlinear aerodynamic effects (Appendix B) will be programmed for solution by various iterative methods.

Another avenue of research will be an attempt to develop a computerizable criterion for the design of airplanes and control systems that will not have jump phenomena in their required maneuver envelope. For example, such a criterion might be based on mathematical constraints on the coefficients of Eqs. (15) or (16), which guarantee the existence of a single real solution.

Appendix A

Response time histories, used for comparison with results of the PSS analysis, were obtained by numerical integration of the equations of motion, assuming constant air density and speed and linear aerodynamics, but inlcuding complete rotational coupling and weight terms. By use of principal axes, these can be written as the following first-order equations, where the "hats" on the moment derivatives indicate that they are defined with the inertia ratios factored out, as shown in Eqs. (A1) to (A3).

$$\dot p = [(I_z - I_y)/I_x](-qr + \hat\ell_\beta\beta + \hat\ell_p p + \hat\ell_r r + \hat\ell_{\delta_a}\delta_a + \hat\ell_{\delta_r}\delta_r) \tag{A1}$$

$$\dot q = [(I_z - I_x)/I_y](pr + \hat m_\alpha \Delta\alpha + \hat m_{\dot\alpha}\dot\alpha + \hat m_q q + \hat m_{\delta_e}\delta_e) \tag{A2}$$

$$\dot r = [(I_y - I_x)/I_z](-pq + \hat n_\beta\beta + \hat n_p p + \hat n_r r + \hat n_{\delta_a}\delta_a + \hat n_{\delta_r}\delta_r) \tag{A3}$$

$$\dot\alpha = q - p\beta + z_\alpha\Delta\alpha + z_{\delta_e}\delta_e + (g/V)\cos\theta\,\cos\phi - \cos\theta_0) \tag{A4}$$

$$\dot\beta = -r\cos\alpha_0 + p(\sin\alpha_0 + \Delta\alpha) + y_\beta\beta$$
$$+ y_{\delta_a}\delta_a + y_{\delta_r}\delta_r + (g/V)\cos\theta\sin\phi \tag{A5}$$

$$\dot\phi = p + q\,\tan\theta\sin\phi + r\,\tan\theta\cos\phi \tag{A6}$$

$$\dot\theta = q\,\cos\phi - r\,\sin\phi \tag{A7}$$

These equations also include the usual assumptions that $\Delta\alpha$ and δ_e are measured from trim values for steady, straight flight, and that $u \approx V$, $\alpha = \alpha_0 + \Delta\alpha \approx w/V$, and $\beta \approx v/V$.

Appendix B

Assuming that the aerodynamic coefficients are nonlinear in α and the control variables, and ignoring the qr term for simplicity, the five equations determining the PSS solutions may be written (where the bars have been dropped for convenience)

$$pq - r\hat n_r(\alpha) - \beta\hat n_\beta(\alpha) = \hat n(\alpha,\delta_a,\delta_r) + p\hat n_p(\alpha) \tag{B1}$$

$$q\hat m_q(\alpha) + pr = -\hat m(\alpha,\delta_e) \tag{B2}$$

$$-q + p\beta = z(\alpha,\delta_e) \tag{B3}$$

$$-r\cos\alpha + \beta y_\beta(\alpha) + p\sin\alpha + y(\alpha,\delta_a,\delta_r) = 0 \tag{B4}$$

$$r\hat l_r(\alpha) + \beta\hat l_\beta(\alpha) + p\hat l_p(\alpha) + \hat l(\alpha,\delta_a,\delta_r) = 0 \tag{B5}$$

The first three equations are linear in q, r, and β, and may be solved for these variables as functions of α, p, and the control variables. The determinant of the governing matrix is a cubic in p and also a function of α.

$$C(p,\alpha) = p^3 - p[\hat n_\beta(\alpha) - \hat m_q(\alpha)\hat n_r(\alpha)] \tag{B6}$$

When the solutions for q, r, and β are substituted into Eq. (B4) and (B5), two nonlinear equations in p and α, are obtained, for given control variables. Remembering that for given control variables the aerodynamic coefficients are all functions of α, the arguments of all of these functions may be dropped for convenience, and the two equations determining the PSS solutions for p and α become

$$y + p\sin\alpha + [1/C(p,\alpha)]\{p^2[(\hat m + \hat m_q\hat n_p)\cos\alpha$$
$$+ y_\beta(z + \hat n_p)] + p\hat n(\hat m_q\cos\alpha + y_\beta)$$
$$+ (z\hat m_q - \hat m)(\hat n_\beta\cos\alpha + \hat n_r y_\beta)\} = 0 \tag{B7}$$

$$\hat l + p\hat l_p + [1/C(p,\alpha)]\{p^2[\hat l_\beta(z + \hat n_p) - \hat l_r(\hat m + \hat m_q\hat n_p)]$$
$$+ p\hat n(\hat l_\beta - \hat l_r\hat m_q) + (z\hat m_q - \hat m)(\hat l_\beta\hat n_r - \hat n_\beta\hat l_r)\} = 0 \tag{B8}$$

Multiplying these through by $C(p,\alpha)$ gives two quartic equations in p.

$$p^4\sin\alpha + yp^3 + p^2[(\hat{m}_q\hat{n}_r - \hat{n}_\beta)\sin\alpha + (\hat{m} + \hat{m}_q\hat{n}_p)\cos\alpha$$
$$+ y_\beta(z+\hat{n}_p)] + p[(\hat{m}_q\hat{n}_r - n_\beta)y$$
$$+ \hat{n}(\hat{m}_q\cos\alpha + y_\beta)] + (z\hat{m}_q - \hat{m})(\hat{n}_\beta\cos\alpha + y_\beta\hat{n}_r) = 0 \quad \text{(B9)}$$

$$\hat{l}_p p^4 + \hat{l}p^3 + p^2[\hat{l}_p(\hat{m}_q\hat{n}_r - \hat{n}_\beta) - \hat{l}_r(\hat{m} + \hat{m}_q\hat{n}_p)$$
$$+ \hat{l}_\beta(z+\hat{n}_p)] + p[\hat{n}(\hat{l}_\beta - \hat{l}_r\hat{m}_q)$$
$$+ \hat{l}(\hat{m}_q\hat{n}_r - \hat{n}_\beta)] + (z\hat{m}_q - \hat{m})(\hat{l}_\beta\hat{n}_r - \hat{l}_r\hat{n}_\beta) = 0 \quad \text{(B10)}$$

These equations may be solved for the PSS values of p and α by some iterative search algorithm, or they may be solved graphically by choosing a set of α values covering a reasonable range and plotting the real p solutions of the two quartic equations vs α. Any crossing points are simultaneous solutions. These solutions then may be substituted into the expressions for $q(p,\alpha)$, $r(p,\alpha)$, and $\beta(p,\alpha)$, whose derivation was described in the preceeding to obtain the complete PSS solution for each specified set of control input values. A computer program is being written to solve these equations, including the qr term.

References

[1]Phillips, W. H., "Effect of Steady Rolling on Longitudinal and Directional Stability," NACA TN 1627, 1948.

[2]Pinsker, W. J. G., "Aileron Control of Small Aspect Ratio Aircraft, in Particular, Delta Aircraft," Aeronautical Research Council Reports and Memoranda 3188, 1953.

[3]Rhoads, D. W. and Schuler, J. M., "A Theroretical and Experimental Study of Airplane Dynamics in Large-Disturbance Maneuvers," *Journal of Astronautical Sciences*, Vol. XXIV, July 1957, pp. 507-526, 532.

[4]Hacker, T. and Oprisiu, C., "A Discussion of the Roll Coupling Problem," *Progress in Aerospace Sciences*, Vol. 15, Pergamon Press, Oxford, 1974.

[5]Haddad, E. K., "Study of Stability of Large Maneuvers of Airplanes," NASA CR-2447, 1974.

[6]Adams, W. M., Jr., "Analytic Prediction of Airplane Equilibrium Spin Characteristics," NASA TN D-6926, 1972.

[7]Etkin, B., *Dynamics of Atmospheric Flight*, Wiley, New York, 1972, pp. 443-451.